Journal of Autoimmunity 103 (2019) 102282

Contents lists available at ScienceDirect

Journal of Autoimmunity

journal homepage: www.elsevier.com/locate/jautimm

# The proteasome activator REGγ counteracts immunoproteasome expression and autoimmunity

Liangfang Yao[a,1], Lei Zhou[a,1], Yang Xuan[a,1], Pei Zhang[b,1], Xiaoshuang Wang[a], Tianzhen Wang[a], Tianyuan Meng[a], Yanyan Xue[a], Xueqing Ma[a], Abdus Saboor Shah[a], Shiwang Shang[a], Xinglong Ma[a], Wei Xie[a], Hao Wang[a], Qing Fu[c], Yanyang Xia[a], Robb E. Moses[d], Hongyan Wang[e], Lei Li[a,****], Jianru Xiao[f,***], Bianhong Zhang[a,**], Xiaotao Li[a,d,*]

[a] Shanghai Key Laboratory of Regulatory Biology, Institute of Biomedical Sciences, School of Life Sciences, East China Normal University, 500 Dongchuan Road, Shanghai, 200241, PR China
[b] Department of Pathology, Chengdu Second People's Hospital, Chengdu, Sichuan, 610017, PR China
[c] Huashan Hospital Affiliated to Fudan University, 12 Middle Wulumuqi Road, Shanghai 200400, PR China
[d] Department of Molecular and Cellular Biology, Baylor College of Medicine, One Baylor Plaza, Houston, TX, 77030, USA
[e] Key Laboratory of Systems Biology, Institute of Biochemistry and Cell Biology, Shanghai Institutes for Biological Sciences, Chinese Academy of Sciences, 320 Yueyang Road, Shanghai, 200031, PR China
[f] Department of Orthopedic Oncology, Changzheng Hospital, The Second Military Medical University, 415 Fengyang Road, Shanghai, 200003, PR China

ARTICLE INFO

*Keywords:*
Autoimmunity
LMP2(7)
Phosphorylated STAT3
REGγ

ABSTRACT

For quite a long time, the 11S proteasome activator REGα and REGβ, but not REGγ, are known to control immunoproteasome and promote antigen processing. Here, we demonstrate that REGγ functions as an inhibitor for immunoproteasome and autoimmune disease. Depletion of REGγ promotes MHC class I-restricted presentation to prime $CD8^+$ T cells *in vitro* and *in vivo*. Mice deficient for *REGγ* have elevation of $CD8^+$ T cells and DCs, and develop age-related spontaneous autoimmune symptoms. Mechanistically, REGγ specifically interacts with phosphorylated STAT3 and promotes its degradation *in vitro* and in cells. Inhibition of STAT3 dramatically attenuates levels of LMP2/LMP7 and antigen presentation in cells lacking REGγ. Importantly, treatment with STAT3 or LMP2/7 inhibitor prevented accumulation of immune complex in $REG\gamma^{-/-}$ kidney. Moreover, $REG\gamma^{-/-}$ mice also expedites Pristane-induced lupus. Bioinformatics and immunohistological analyses of clinical samples have correlated lower expression of REGγ with enhanced expression of phosphorylated STAT3, LMP2 and LMP7 in human Lupus Nephritis. Collectively, our results support the concept that REGγ is a new regulator of immunoproteasome to balance autoimmunity.

## 1. Introduction

Defects in the peptide processing machinery perturb the formation of MHC class I complexes and their recognition by $CD8^+$ T cells that are crucial for pathogen eradication [1] and tumor immunosurveillance [2]. $CD8^+$ T cells and Dendritic cells (DCs) have also been implicated to play pivotal roles in autoimmune diseases [3–5]. In systemic lupus erythematosus (SLE) patients, there is increased expression of costimulatory molecules CD40/CD86 on DC [4]. In multiple scleroses (MS), experimental autoimmune encephalomyelitis (EAE), and immune thrombocytopenia, the number of $CD8^+$ T cells are expanded [6–10]. Conversely, depletion of $CD8^+$ T cells reduces the severity of disease in experimental autoimmune glomerulonephritis, experimental autoimmune myasthenia gravis and several rheumatoid arthritis (RA) models [5,11]. These studies highlight the importance of DC and $CD8^+$ T cells in the initiation of autoimmune diseases.

The proteasome is a multi-subunit protease complex. The 20S core of the complex is composed of four heptameric rings with a barrel-

* Corresponding author. Department of Molecular and Cellular Biology, Baylor College of Medicine, One Baylor Plaza, Houston, TX 77030, USA.
** Corresponding author.
*** Corresponding author.
**** Corresponding author.
*E-mail addresses:* lllkzj@163.com (L. Li), jianruxiao83@163.com (J. Xiao), bhzhang@bio.ecnu.edu.cn (B. Zhang), xiaotaol@bcm.edu (X. Li).
[1] These authors contributed equally to this work.

https://doi.org/10.1016/j.jaut.2019.05.010
Received 9 March 2019; Received in revised form 10 May 2019; Accepted 14 May 2019
Available online 04 June 2019

shaped structure. The two outer rings are identical and each contain seven distinct α subunits (α1-α7). The two inner rings are also identical and each contains seven different β subunits (β1-β7) [12]. The proteolytic activity resides in three of the β subunits, β1, β2 and β5. These three subunits are replaced by functionally different counterparts named low molecular weight protein (LMP)2 (also called β1i), LMP7 (β5i) and multi-catalytic endopeptidase complex-like (MECL)1 (β2i), respectively in the immunoproteasome [13,14]. LMP2, LMP7 and MECL1 are induced in the majority of cells by pro-inflammatory cytokines such as type I IFN (α, and β) and type II IFN (γ) or TNF [15,16], whereas they are constitutively expressed in immune cells [17]. Accumulating evidence demonstrates the importance of the immunoproteasome in autoimmune diseases. *LMP2*$^{-/-}$ *MECL1*$^{-/-}$ *LMP7*$^{-/-}$ knock-out mice have a marked decrease in the generation of MHC class I ligands [18]. Inhibition of the immunoproteasome ameliorates symptoms in various mouse models of autoimmune diseases, such as RA [19], SLE [20], Hashimoto's thyroiditis [21], and MS [22].

The activity of the proteasome is greatly enhanced by three classes of proteasome activator complexes: PA700 (or 19S) activator; PA200; and PA28 (or 11S) family members [23]. REGα, REGβ and REGγ (also known as PA28γ, PSME3, and Ki) are 11S family members. REGα and REGβ form a hetero-heptamer and are mainly located in cytoplasm. They can be induced by IFNγ to participate in processing of specific antigens [24–26]. In contrast, REGγ expression is decreased upon IFNγ stimulation [25], and is predominantly distributed in the nucleus as homo-heptamer. REGγ has been known to direct proteasomal degradation of numerous intact proteins, including SRC3 [27], p21 [28,29], p16 [29], p19/p14 [29], activation-induced deaminase (AID) [30], and CK1 [31], establishing the function of REGγ in a variety of cellular processes. The synchronized diverse regulation of REGα/β and REGγ by IFNγ may suggest an opposite function of REGγ in the regulation of immunoproteasome and antigen presentation. Therefore, it is worth investigation whether REGγ plays a role in the regulation of antigen processes.

In this study, we demonstrate that REGγ modulates immunoproteasome expression and function during antigen processing in a phospho-STAT3 dependent manner. Mice deficient for *REG*γ develop spontaneous autoimmune symptoms with age. Clinical implication of REGγ in the formation of Lupus nephritis indicates that the REGγ-proteasome represents a novel inhibitory pathway to restrain over-activation of immunoproteasome and consequential development of autoimmune diseases.

## 2. Material and methods

### 2.1. Experimental mice

*REG*$\gamma^{-/-}$ mice (C57BL/6 genetic background) were acquired from Dr. John J. Monaco. To generate the homologous mice for our study, we maintained *REG*$\gamma^{\pm}$ mice intercrossed for over 10 generations. The genotypes of *REG*$\gamma^{+/+}$ and *REG*$\gamma^{-/-}$ mice were identified by PCR. Age and gender-matched mice were used in all experiments. For pristane induced lupus-like phenotype, 3-month-old age- and gender-matched *REG*$\gamma^{+/+}$ and *REG*$\gamma^{-/-}$ female mice were administered intraperitoneally with 0.5 mL of pristane (2, 6, 10, 14-tetramethylpentadecane) (Sigma-Aldrich). 200–500 μL urine or 50–100 μL blood was collected with an interval of 1 month for experiment. Mice were sacrificed at 6 months after pristane injection. Immunological and pathological characters were assessed.

### 2.2. Plasmids and reagents

pCMV-Tag2B-STAT3, pCMV-Tag2B-STAT3 (Y705F), pCMV-Tag2B-STAT3 (Y705D), pSG5-HA-STAT3, pSG5-HA-STAT3 (Y705F), pSG5-HA-STAT3 (Y705D), pcDNA3.1-p21, pGL3-basic-LMP2, pGL3-basic-LMP7, and pGL3-basic-MECL1 reporter genes were constructed by following standard molecular cloning technology. All the constructs were confirmed by DNA sequencing.

The information of antibodies used in Western blotting, ChIP, immunofluerence (IF) and IHC experiments were as follows: STAT1, p-STAT1, p-STAT3, STAT5, p-STAT5, STAT6, p-STAT6, LMP2, LMP7, CD11c, and REGγ (Abcam); STAT3, (Cell Signaling Technology); IgA, IgG, and C3 (Bioss); MECL1 (Santa Cruz Biotechnology); p21 (BD Pharmingen); IgG, Flag, HA, β-Actin, protein A/G beads, Flag-M2 beads, and HA-beads (Sigma-aldrich). PR-957, and Dox were purchased from Biotool company; OVA, OVA (257–264), OVA (323–339), IFNγ and Cucurbitacin E were purchased from Sigma-aldrich. ELISA kits for IgA, IgG, IgM, and ANA detection were purchased from eBioscience, Albuminuria, BUN, and Cr detection kits were from Nanjing Jiancheng.

The STAT3 siRNA sequence was as follows: 5′- CCACTTTGGTGTT TCATAA-3'. The control siRNA sequence was UUCUCCGAACGUGUCA CGUdTdT.

### 2.3. Cell culture and treatments

293T was purchased from ATCC; 293WT, 293-*REG*γ (WT) inducible cells, were generated as described previously [32]; BMDC, and Splenic DC were isolated from *REG*$\gamma^{+/+}$ and *REG*$\gamma^{-/-}$ mice; $CD8^+$ T, $CD4^+$ T cells were isolated from transgenic OT-I or OT-II mice. DC, $CD8^+$ T, $CD4^+$ T cells were cultured in 1640 (Gibco) supplemented with 10% fetal bovine serum (FBS), penicillin (50U/mL) and streptomycin (50 μg/mL), other cells were cultured in full DMEM. Cells were transfected with Lipofectamine 2000 (Invitrogen) according to the manufacturer's instructions. For cell treatments, 25 ng/mL IFNγ, 250 nM Cucurbitacin E, 100 μg/mL CHX, or 10μmol/L Doxycycline (Dox) was used.

Bone marrow–derived DCs (BMDCs) were generated from mouse (6–8 weeks old) femur bone marrow suspensions by depletion of red cells, and then were cultured in RPMI 1640 medium supplemented with 10% FBS, rmGM-CSF (10 ng/mL) and rmIL-4 (1 ng/mL). Non-adherent cells were gently washed out on day 3 of culture; The remaining loosely adherent clusters were cultured for 4 days in the presence GM-CSF and IL-4. At day 7, cells were positively selected using CD11c magnetic microbeads for experiment. Splenic DC cells were isolated from *REG*$\gamma^{+/+}$ and *REG*$\gamma^{-/-}$ mice by using CD11c magnetic microbeads.

### 2.4. In vitro co-cultures and in vivo cell transfers

$CD8^+$ T cells or $CD4^+$ T cells were isolated from the spleens of 8 weeks old OT-I or OT-II mice using MACS negative selection kits. T cells ($2 \times 10^7$ cells/mL) were labeled with CFSE. For *in vitro* assay, BMDC from WT or *REG*$\gamma^{-/-}$ mice were incubated for 3 h with OVA or different OVA peptides, and then co-cultured with OT-I or OT-II T cells for 3 days. Cells were fixed with 2% PFA in PBS for 15 min at room temperature, followed by FACS analysis. For *in vivo* assay, CFSE-labeled T cells were injected into WT or *REG*$\gamma^{-/-}$ mice by tail vein, followed by OVA immunization. Then the Draining Lymph Node analysis was performed by FACS.

### 2.5. Immunoprecipitation and western blotting

Cells were harvested and lysed in pre-cooled lysis buffer (50 mM Tris-HCl, pH7.5, 1 mM EDTA, 150 mM NaCl, 1% NonidetP-40, 10% glycerol and protease inhibitors) for 30 min on ice then centrifuged for 10 min at 12 000 r.p.m. For immunoprecipitation assay, 5 μL flag beads or 10 μL protein A/G beads with 3 μL specific primary antibody was added to 600 μL whole cell lysates, and then incubated for 4 h at 4 °C. Immunoprecipitates were washed 4 times with lysis buffer. The pellet was then subjected to electrophoresis in 10% SDS polyacrylamide-gel. After blocking, samples were incubated with specific primary antibodies at 4 °C overnight, washed and incubated for 1 h with secondary antibodies, then washed 3 more times and visualized by Odyssey LI-COR-scanner.

### 2.6. In vitro protein degradation assay

Recombinant REGγ protein and 20S were purified. The substrate STAT3(Y705D) and STAT3(Y705F) protein was generated by *in vitro* translation of TNT kit (Promega). The target protein decay assay was subsequently performed by incubating substrate, 20S proteasome and REGγ heptamers for 2 h in 25 μL reaction volume at 30 °C with appropriate controls. The results were analyzed by immunoblotting and were repeated at least three times.

### 2.7. Reverse Transcription-quantitative PCR

Total RNA was extracted from cells using Trizol (Takara), following the manufacturer's instruction. 1 μg of total RNA was reverse-transcribed to cDNA. The quantification of gene transcripts was performed by real time PCR using a master-mix with SYBR-green (Toyobo). Each experiment was performed in duplicates and was repeated at least three times. Relative expression was calculated using 18S as an endogenous control. The primers were as follows: 18S sense, 5′-TTCCGATAACGA ACGAGACTCT-3′; antisense, 5′-TGGCTGAACGCCACTTGTC3'; LMP2 sense, 5′-GGGACAACCATCATGGCAGT3′; antisense, 5′-CAGCAGCGGA ACCTGAGAG-3′; LMP7 sense, 5′- ATGGCGTTACTGGATCTGTGC-3′; antisense, 5′-GCGGAGAAACTGTAGTGTCCC-3′; MECL1 sense, 5′-GAG GAATGCGTCCTTGGAACA-3′; antisense, 5′-CACAACCGAATCGTTAGT GGC-3′; STAT3 sense, 5′- CAATACCATTGACCTGCCGAT-3′; antisense, 5′- GAGCGACTCAAACTGCCCT-3′;

### 2.8. Immunofluorescence staining (IF)

Cells were seeded onto sterile coverslips at indicated times. Cover slips with the cells were washed once with PBS and fixed in 4% formalin for 10 min. Cells were permeabilized and blocked for 30 min at room temperature in a staining buffer containing Triton X-100 (0.1%) and BSA (2%) followed by incubation with primary antibody in 2% BSA overnight at 4 °C. After washing three times in PBS, cells were incubated with Cy3- or FITC-conjugated anti-mouse for 1 h at room temperature and then with DAPI for 10 min. The cover slips were then washed extensively and fixed on slides. Imaging of the cells was carried out using fluorescence microscopy.

### 2.9. Luciferase assay

After transfection and/or treatment, the cells were washed with PBS for 3 times. The cells were then lysed in the luciferase lysis buffer provided with the luciferase Assay Kit (Promega, Madison, USA). Then the whole cell lysates were centrifuged at 12 000 rpm for 10 min. Supernatant was collected and added to luciferase assay substrate following instructions. Luminescence was measured. Each assay was repeated for at least three times.

### 2.10. Chromatin Immunoprecipitation assay

After mock or Cue treatment, formaldehyde was added directly to the medium to a final concentration of 1% for 10 min. Then glycine was added to a final concentration of 0.125 M and incubated for 5 min at room temperature. The cells were washed twice with ice cold PBS, lysed the cells in lysis buffer [1% SDS, 10 mM EDTA, protease inhibitors and 50 mM Tris-HCl (pH 8.1)] and the lysates were sonicated. After centrifugation, the lysates were diluted in ChIP dilution buffer [0.01% SDS, 1.0% Triton X-100, 1.2 mM EDTA, 16.7 mM NaCl, protease inhibitors and 16.7 mM Tris-HCl (pH 8.1)]. The chromatin resuspension was incubated with a salmon sperm DNA/protein A agarose slurry for 30 min at 4 °C with agitation. The recovered chromatin solutions were incubated with 3–5 μg of indicated antibodies overnight at 4 °C. 60 μL of protein A agarose slurry was added for 2 h at 4 °C with rotation. The beads were washed sequentially for 5 min with the following buffers: low salt wash buffer [0.1% SDS, 1% Triton X-100, 2 mM EDTA, 150 mM NaCl and 20 mM Tris–HCl (pH 8.1)], high salt wash buffer [0.1% SDS, 1% Triton X-100, 2 mM EDTA, 500 mM NaCl and 20 mM Tris–HCl (pH 8.1)] and LiCl wash buffer [0.25 mM LiCl, 1% Nonidet P-40, 1% sodium deoxycholate, 1 mM EDTA and 10 mM Tris–HCl (pH 8.1)]. Finally, the beads were washed twice with 1 mL TE buffer. Elution buffer (1% SDS and 100 mM $NaHCO_3$) were added and the supernatant made to final concentration of 200 mM NaCl and incubated overnight at 65 °C. Proteinase K (40 μg/mL) was added and incubated for 1 h at 45 °C. The DNA was recovered and precipitated. PCR was performed with specific primers and the PCR products were separated by electrophoresis through 2% agarose gel.

### 2.11. Immune cell population analysis

Spleens from WT, *REGγ*$^{-/-}$ mice were ground in 4 mL of MACS buffer. Splenocyte cell suspensions were made in 1–2 mL of red blood cell lysis buffer (Biolegend), washed in PBS and pelleted (1500 rpm, 5 min). 1 x $10^6$ splenocytes were added per FACS tube. Splenocytes were fixed with 2% PFA in PBS for 15 min at room temperature, and incubated with indicated antibody for 30 min in dark followed by FACS analysis.

### 2.12. Tissues histology and IHC (immunohistochemsitry)

The tissues were fixed in 4% buffered formalin, Paraffin embedded sections were de-paraffined with xylene and dehydrated with sequential washes of 100%, 95% and 70% ethanol, followed by 3% hydrogen peroxide in methanol for 30 min to quench the endogenous peroxidase activity, and then washed in phosphate buffered saline (PBS). Then samples were boiled to achieve antigen retrieval in retrieval solution (pH 6), at 100 °C for 30 min, followed by a cool down period to room temperature. For tissue histology analysis, 4-μm paraffin sections were stained with hematoxylin and eosin (H&E), and Masson's trichrome (MT) stain. According to the damaging of tubules, glomerulosclerosis, capillary loop and mononuclear infiltration of kidney, the statistical analysis of pathology disorder was evaluated score: 0, 1, 2, 3, 4. For IHC analysis, slides were incubated with indicated primary antibodies at 4 °C overnight, then washed in PBS three times and incubated with secondary antibodies for 1 h at room temperature. After washing three times with PBS, slides were stained with 3, 3′-diaminobenzidine. For statistical analysis, staining intensity was evaluated as follows: 0 and rated as negative (−), weak staining (+), moderate/strong staining (++) and very strong staining (+++).

### 2.13. ELISA

IgA, IgG, IgM, ANA, Albuminuria, BUN, SCr were analyzed by ELISA kits according to the manufacturer's instructions. Data represent mean ± SEM (error bars) of at least three independent experiments.

### 2.14. Bioinformatics analysis

Raw data were downloaded from NCBI Gene Expression Omnibus (GEO, http://www.ncbi.nlm.nih.gov/geo) database (ID:GSE32591). Samples in datasets were grouped into two groups: the healthy normal group (n = 14), and patients with lupus nephritis(LN) (n = 32). The data were processed by R packages of arrayQualityMetrics and affyQCReport (http://www.r-project.org/). All the datasets mentioned above were passed through QC (Quality control). Collected data were normalized by robust multi-array average (RMA) and expression measured depending on affy packages in R. The log2 ratios of gene expression values were calculated and used in all subsequent analyses. The one-way ANOVA method was used to analyze the mean of the two groups. Bonferroni method was used to adjust p value in paired t-test. All statistical analysis was performed in R.

### 2.15. Statistics

Prism software (GraphPad Software) was used for statistical analyses. Values are shown as mean ± S.E.M. Statistical significance between two samples was determined with two-tailed Student's t-test.

### 2.16. Study approval

All animal experiments complied with the National Institutes of Health guide for the care and use of Laboratory animals (NIH Publications No. 8023, revised 1978). Experiments for human samples had been carried out in accordance with The Code of Ethics of the World Medical Association (Declaration of Helsinki) for experiments involving humans. All studies were reviewed and approved by IACUCs of East China Normal University.

## 3. Results

### 3.1. Loss of REGγ promotes expression of immunoproteasome catalytic subunits

Although REGα/β, in specific antigen processing, does not alter expression of immunoproteasome subunits [24,33], it remains to be determined if REGγ does. Although previous studies reported no significant differences in the expression of immunoproteasome subunits in multiple tissues between WT and *REGγ*$^{-/-}$ mice, there was no detailed examination in antigen presenting cells [34]. In our study, we analyzed the protein expression profile of immunoproteasome subunits in several cells including isolated DCs where immunoproteasome is highly enriched. Results showed significantly higher LMP2, LMP7, and slightly higher MECL1 levels in REGγ depleted BMDC (Fig. 1A), splenic DC (sDC) (Fig. 1B), MEF and HeLa cells (Fig. S1A) than in corresponding WT cells. Reverse Transcription-quantitative PCR (RT-qPCR) analysis suggested an enhanced transcription of *Lmp2* and *Lmp7*, but not *Mecl1*, in *REGγ*$^{-/-}$ BMDC (Fig. 1C), splenic DC (Fig. 1D), and MEF cells compared to WT (Fig. S1B), indicating that REGγ negatively regulates expression of catalytic subunits of the immunoproteasome.

### 3.2. REGγ deficiency enhances MHC-I restricted antigen processing and presentation

Since immunoproteasome plays a crucial role in antigen processing and autoimmune diseases, we tested whether REGγ affects antigen processing and presentation ability of DC *in vitro*. CD8$^+$ MHC I-restricted T cells (from OT-I mice) and CD4$^+$ MHC II-restricted T cells (from OT-II mice) were purified and labeled with 5(6)-Carboxyfluorescein diacetate N-succinimidyl ester (CFSE), then co-cultured with ovalbumin (OVA)- or OVA peptide-pulsed WT or *REGγ*$^{-/-}$ BMDC for 3 days. Notably, with the presence of OVA protein, the proliferation of CD8$^+$ T cell that co-cultured with REGγ-deficient BMDC was significantly increased in a range of antigen doses, compared to that with WT BMDC (Fig. 2A). However, comparable CD8$^+$ T cell proliferation were observed in the presence of WT or *REGγ*$^{-/-}$ BMDC stimulated with OVA$_{(257-264)}$ peptide (Fig. 2B), suggesting that REGγ-dependent regulation of antigen presentation mainly affects antigen processing, not antigen uptake or delivery. In contrast, similar proliferation rates were observed for CD4$^+$ T cells co-cultured with either *REGγ*$^{+/+}$ or *REGγ*$^{-/-}$ BMDC following OVA or OVA$_{(323-339)}$ peptide stimulation (Fig. S2A and B), indicating that REGγ doesn't participate in regulation of MHC-II restricted antigen presentation in this study. To substantiate the regulatory function of REGγ in antigen presentation *in vivo*, we transferred purified and CFSE-labeled OT-I CD8$^+$ T cells into WT and *REGγ*$^{-/-}$ mice and then immunized with OVA or OVA$_{(257-264)}$ peptide using a range of doses. Consistent with *in vitro* results, *REGγ*$^{-/-}$ mice showed higher donor CD8$^+$ T cell proliferation than WT after OVA immunization (Fig. 2C), whereas the proliferation were comparable after the challenge with OVA$_{(257-264)}$ peptide (Fig. 2D). WT and *REGγ*$^{-/-}$ mice transplanted with OT-II CD4$^+$ T cells had no difference in proliferation after OVA stimulation (Fig. S2C). Notably, immune cell population analysis showed that the CD11c$^+$ and CD8$^+$ T cell percentage and numbers were significantly increased in the spleen of 12-month-old REGγ-deficient mice but not in 3-month-old mice (Fig. 2E and data not shown). No significant differences were found in CD4$^+$, CD19$^+$, and CD11b$^+$ cells between the *REGγ*$^{-/-}$ mice and the WT littermates at any age (Fig. 2E). Our results suggest that REGγ primarily regulates MHC I-restricted, but not MHC II-restricted, antigen processing, and eventually affects proliferation of CD8$^+$ T cells.

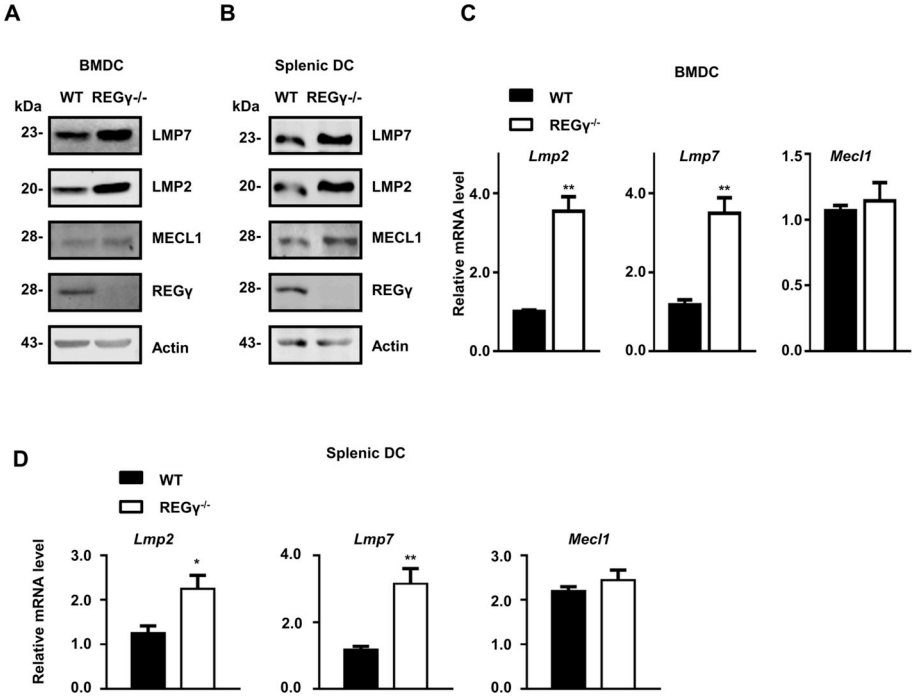


**Fig. 1. REGγ deficiency promotes the expression of immunoproteasome catalytic subunits.** Immunoproteasome subunits in BMDC **(A),** and splenic DC **(B)** purified from *REGγ*$^{+/+}$ and *REGγ*$^{-/-}$ mice were analyzed by western blotting with indicated antibodies. Data are repeated more than five times. The mRNA levels of immunoproteasome subunits in BMDC **(C)** and sDC **(D)** were detected by Reverse Transcription-quantitative PCR. Data are shown as mean ± SEM from three independent experiments. **p < 0.01 (two-tailed Student's t-test).

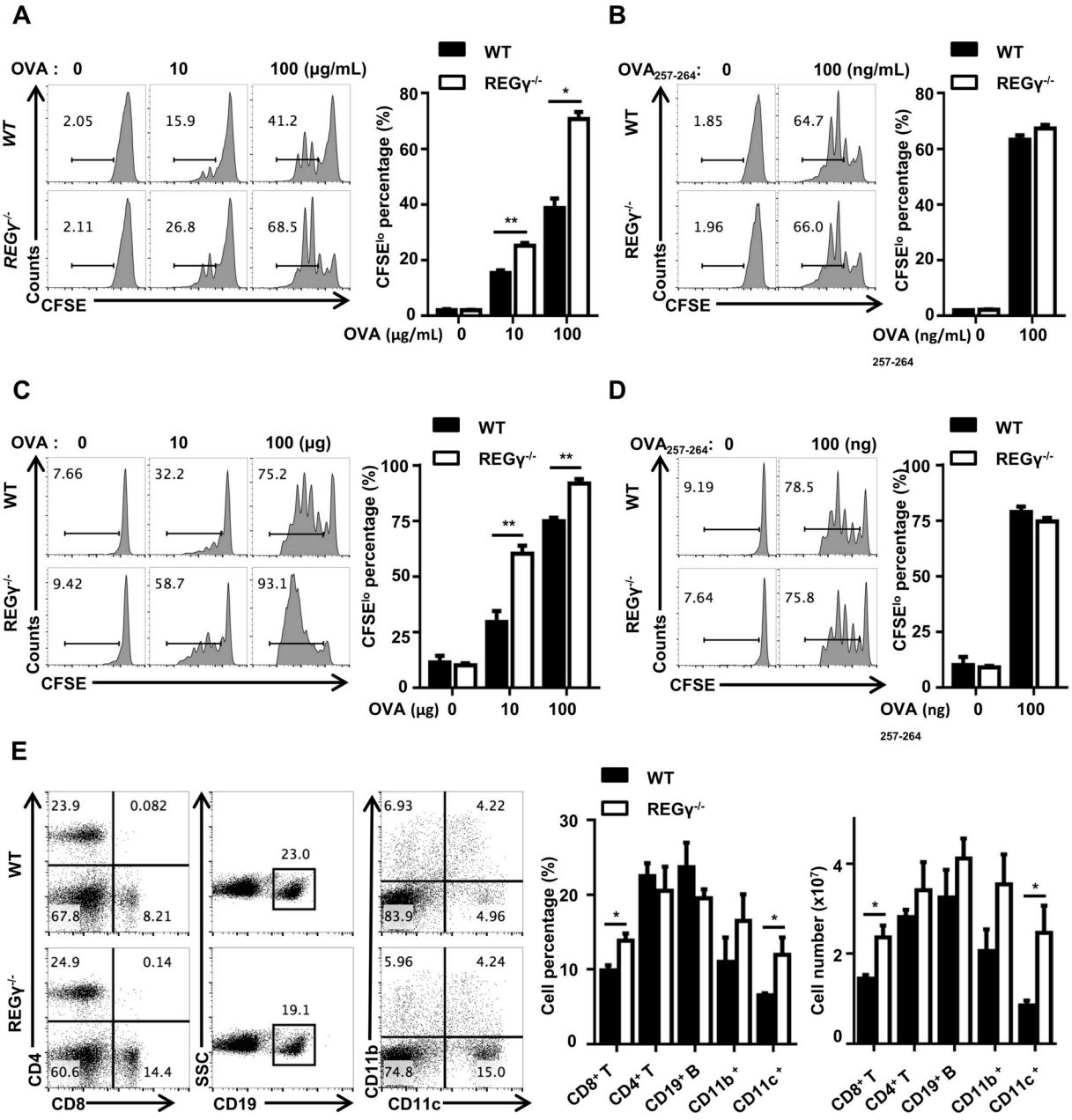


**Fig. 2. REGγ deficiency enhances MHC-I restricted antigen processing and presentation. (A, B)** The proliferation of purified and CFSE-labeled $CD8^+$ T cells from 6 to 8 week OT-I mice was measured by flow cytometry after co-culture 3 days with indicated concentration of OVA **(A)** or OVA $_{(257\text{-}264)}$ peptide-pulsed **(B)** WT or *REG*$\gamma^{-/-}$ BMDC. (n = 5 cultures for each group). **(C, D)** The proliferation of $CD8^+$ T cells *in vivo*. Purified and CFSE-labeled OT-I $CD8^+$ T cells were transferred into WT and *REG*$\gamma^{-/-}$ mice via tail vein injection and then immunized with indication doses of OVA **(C)** or OVA $_{(257\text{-}264)}$ peptide **(D)** by intraperitoneal injection. After 3 days, the immunized mice were sacrificed and inguinal LNs were collected for analysis. (n = 6 mice for each genotype). **(E)** Flow cytometry analysis of immune cell population in the spleen of 12-month-old *REG*γ WT or *REG*γ KO mice. (n = 6 mice for each genotype). Flow cytometry plots was based on splenocytes single cells. Quantitative results of flow cytometry from three independent experiments are shown. *p < 0.05 and **p < 0.01 (two-tailed Student's t-test). Error bars represented ± SEM.

### *3.3. REGγ-deficient mice develop spontaneous autoimmune symptom with age*

Pharmacological inhibition or genetic ablation of immunoproteasome could change antigen presentation and autoimmunity [18,20], however, it remains unknown if autoimmune symptoms may develop when immunoproteasome is hyperactivated in mice lacking *REG*γ. The kidney is a highly vascular organ and vulnerable to autoimmune-mediated injury [35]. Thus we inspected the changes in renal tissue in aging mice since compensation of trypsin-like activity by other proteasome in *REG*γ KO mice is diminished with age [36]. Dissection of kidneys showed glomerular sclerosis and interstitial fibrosis in 12-month and 18-month aged *REG*$\gamma^{-/-}$ mice versus age matched WT mice, whereas 3-month-old *REG*$\gamma^{-/-}$ kidneys and age-matched *REG*$\gamma^{+/+}$ controls were almost histologically normal. (Fig. 3A and B, Fig. S3A). Accordingly, serum levels of blood urea nitrogen (BUN) and serum creatinine (Cr) were significantly higher in both 12-mon-old ($p < 0.05$) and 18-mon-old ($p < 0.01$) *REG*$\gamma^{-/-}$ mice, but unchanged in 3-mon-old animals (Fig. S3B). Immunofluorescence (IF) staining indicated more dramatic infiltration of immunocytes in *REG*$\gamma^{-/-}$ renal tissues (Fig. 3C), with co-staining of $CD11c^+$ and immunoproteasome markers in both 3- and 18-mon-old kidneys (Fig. S3C). Age-dependent

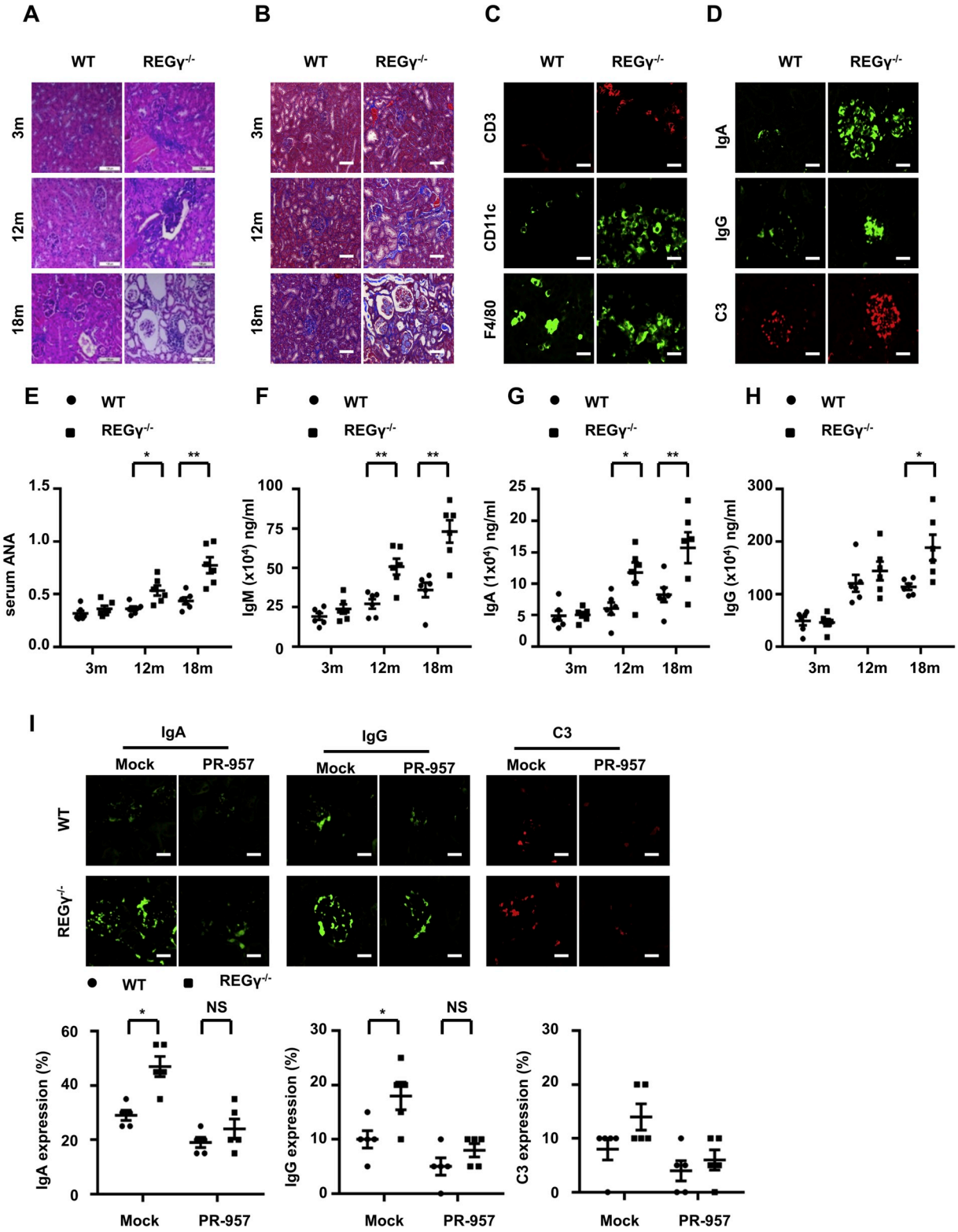


**Fig. 3.** ***REG*γ deficient mice display age-related autoimmune symptoms.** **(A)** H&E and **(B)** Masson Trichrome staining of kidney sections from $REG\gamma^{+/+}$ and $REG\gamma^{-/-}$ mice at indicated age. Magnification: 20x. Bar = 100 μm. **(C)** Immunofluorescence staining with indicated antibodies (CD3, CD11c and F4/80) to detect infiltration of immunocytes in kidney tissues from 18-month-old $REG\gamma^{+/+}$ or $REG\gamma^{-/-}$ mice. Magnification: 40x. Bar = 50 μm. **(D)** IF staining with anti-IgA, IgG and Complement C3 in kidneys from 18-month-old $REG\gamma^{+/+}$ or $REG\gamma^{-/-}$ mice. Magnification: 40x. Bar = 50 μm. **(E-H)** Serum levels of ANA, IgM, IgA and IgG in $REG\gamma^{+/+}$ and $REG\gamma^{-/-}$ mice at indicated age were detected by ELISA. (n = 6 mice for each group). **(I)** 9-month-old wild type or $REG\gamma^{-/-}$ mice were treated with PR-957 (5 mg/kg) every two weeks for 3 months and kidneys were sectioned for immunofluorescence staining. Magnification: 40x. Bar = 50 μm. Lower panel showed the statistic results, *p < 0.05. (n = 5 mice for each genotype). Data are shown as mean ± SEM. *p < 0.05, **p < 0.01 (two-tailed Student's t-test).

**Table 1**
Antibody array results for indicated gene expression change in *REGγ*$^{-/-}$ versus *REGγ*$^{+/+}$ MEF cells.

| Name | Fold Change | T-test |
|---|---|---|
| STAT3(Tyr705) | 1.682 | 0.00620 |
| STAT1(Tyr701) | 0.874 | 0.0380 |
| STAT5(Tyr694) | 1.268 | 0.126 |
| STAT6(Tyr641) | 0.822 | 0.185 |
| JAK1(Tyr1022) | 1.507 | 0.133 |
| JAK2(Tyr221) | 1.239 | 0.157 |

glomerular depositions of immunoglobulin A (IgA), IgG and complement component 3 (C3) proteins in REGγ-deficient kidneys were detected (Fig. 3D and Fig. S3D-F). Consistently, serum levels of ANA, IgM, IgA and IgG were markedly increased in aged *REGγ*$^{-/-}$ mice compared with *REGγ*$^{+/+}$ counterparts (Fig. 3E–H). More importantly, PR-957, an inhibitor of LMP2/LMP7, could reverse the IgA, IgG and C3 depositions in kidney of 12-mon-old REGγ-deficient mice by varying degrees (Fig. 3I). These results suggest that REGγ deficiency may promote spontaneous autoimmune symptoms in a LMP2/7-dependent manner in aged mice.

### 3.4. Tyrosine (705)-phosphorylated STAT3 is regulated by REGγ

JAK-STAT pathway is known to regulate the transcription of immunoproteasome subunits [37]. To determine the molecular target(s) of REGγ, we performed a high-throughput proteomic screen against antibody arrays (FullMoon BioSystems) [38]. Among the candidate proteins in the JAK-STAT pathways, only Tyr (705)-p-STAT3 (referred to as p-STAT3), but not other STAT family members, was significantly higher in *REGγ* depleted cells than in WT (Table 1). To validate this, we examined the expression of STAT1/3/5/6 and their phosphorylated forms in WT and *REGγ* deficient cells. Only p-STAT3 was consistently increased in *REGγ*$^{-/-}$ BMDC (Fig. 4A), *REGγ*$^{-/-}$ MEF cells (Fig. S4A and B) and HeLa *shR* cells (Fig. S4A). Since REGγ is mainly in the nucleus and STAT3 is translocated into the nucleus upon phosphorylation [39,40], we evaluated the stability of nuclear-localized p-STAT3. Immunofluorescence analysis displayed nuclear accumulation of p-STAT3 in both *REGγ*$^{-/-}$ BMDC (Fig. 4B) and HeLa *shR* cells (Fig. S4C). However, we found no changes in JAK1/2 or their phosphorylated forms in BMDC (Fig. 4C), and HeLa cells (Fig. S4D), suggesting that REGγ does not affect components upstream of STAT3. Due to unchanged mRNA levels of STAT3 between WT and *REGγ*$^{-/-}$ BMDC (Fig. 4D), our data indicate that REGγ regulates stability of p-STAT3.

### 3.5. REGγ interacts with p-STAT3 and promotes its degradation

To determine the dynamic regulation of REGγ for p-STAT3 stability, we treated *REGγ*$^{+/+}$ and *REGγ*$^{-/-}$ BMDC with cycloheximide (CHX) and performed Western blotting analysis of STAT3 and p-STAT3. P-STAT3 decayed faster in *REGγ*$^{+/+}$ than in *REGγ*$^{-/-}$ BMDC. However, there was no difference in degradation rate for total STAT3 (Fig. 5A and B). Similar dynamic changes for STAT3 and Tyr (705)-p-STAT3 were observed in CHX-treated HeLa *shN* and HeLa *shR* cells (Fig. S4E). Reciprocal immunoprecipitation analysis revealed physical interaction between endogenous REGγ and p-STAT3 in BMDC (Fig. 5C) and MEF cells (Fig. S4F).

To test the importance of Tyr (705) p-STAT3 in REGγ-mediated degradation, we constructed phosphor-mimetic (STAT3-Y705D) and phosphor-defective (STAT3-Y705F) mutations, followed by analysis of their degradation dynamics in 293 inducible cells. With doxycycline induced expression of REGγ, STAT3-Y705D displayed faster degradation than in non-induced control cells (Fig. 5D), while no changes in degradation rate of STAT3-Y705F were observed before and after doxycycline induction (Fig. S4G). Consistent with this, STAT3-Y705D, but not STAT3-Y705F, was able to interact with REGγ (Fig. 5E). To substantiate p-STAT3 as a direct target of REGγ, we performed *in vitro* proteolytic analysis using purified REGγ and 20S. Incubation of *in vitro* translated STAT3-Y705D with inactive 20S proteasome or REGγ alone exhibited no significant degradation beyond non-specific decay. However, a combination of REGγ and 20S proteasome promoted marked degradation of STAT3-Y705D and p21 (as a positive control), but not STAT3-Y705F, in the absence of additional ATP (Fig. 5F). These results

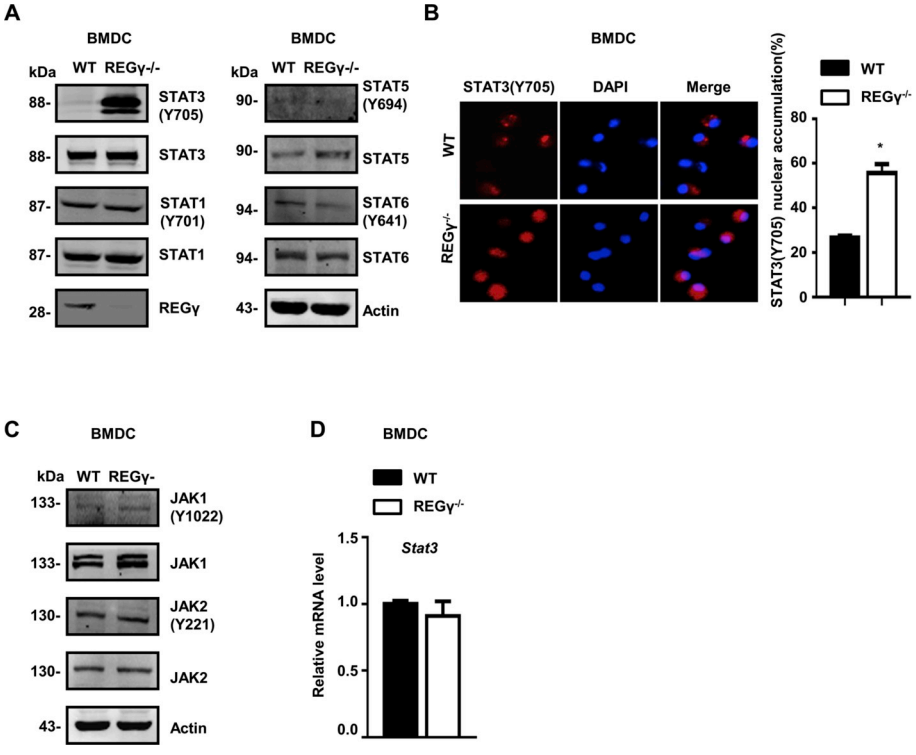


**Fig. 4. Lack of REGγ leads to an elevated protein level of phosphorylated-STAT3. (A)** BMDC from WT or *REGγ*$^{-/-}$ mice was lysed and Western blotting were performed using indicated antibodies. Experiments were repeated at least 10 times. **(B)** The nucleus-localized phospho-STAT3 in BMDC from WT or *REGγ*$^{-/-}$ mice was detected by immunofluorescence staining. The bar graph shows the quantitative analysis of subcellular localization of p-STAT3. Magnification: 40×. **p < 0.01 (two-tailed Student's t-test). Experiments were repeated at least 3 times. **(C)** Cell lysates from WT or *REGγ*$^{-/-}$ BMDC were used for Western blotting analysis using indicated antibodies. Data are repeated more than five times. **(D)** Total RNA was extracted from 3-month-old mice BMDC and analyzed by Reverse Transcription-quantitative PCR. Experiments were repeated more than five times.

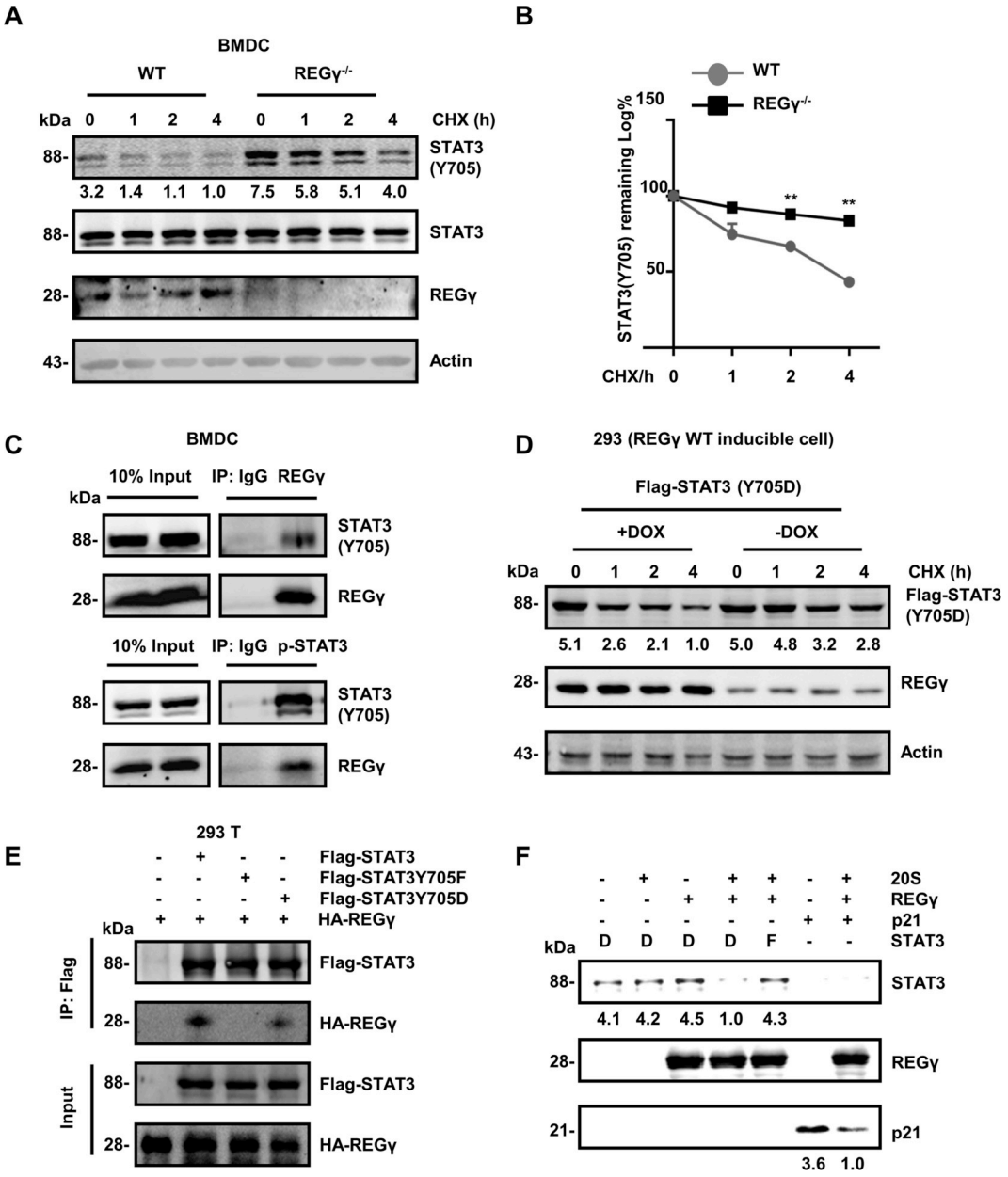


**Fig. 5. REGγ promotes the degradation of Tyr(705) phosphorylated STAT3. (A)** BMDC cells from *REG*γ WT or KO mice were treated with CHX (cycloheximide, 100 μg/mL) for indicated times and followed by Western blotting analysis. **(B)** Experiments in **(A)** were repeated for 3 times to do statistical analysis. **p < 0.01 (two-tailed Student's t-test). **(C)** Immunoprecipitation was performed with whole cell lysates of BMDC using anti-REGγ or anti-Y705-p-STAT3 antibodies. The immunoprecipitated complexes were subjected to SDS-PAGE and detected by indicated antibodies. Representative image was shown. **(D)** 293 inducible REGγ(WT) expressing cells were transiently transfected with STAT3(Y705D) and treated with or without doxycycline for 36 h, then CHX (100 μg/mL) was added for indicated time periods. The stability of STAT3 (Y705D) was measured by Western blotting. **(E)** 293T cell lines were co-transfected with indicated plasmids and then subjected to immunoprecipitation with conjugated anti-Flag beads. Samples were analyzed by Western Blotting using indicated antibodies. **(F)** *In vitro*-translated STAT3(Y705D), or STAT3(Y705F) or p21 (as positive control) were incubated with purified REGγ, or 20S proteasome alone or combined, followed by Western blotting analysis. In **(D-F)**, experiments were repeated for three times.

show that, Tyr (705)-phosphorylated STAT3 is a direct substrate of REGγ.

### *3.6. REGγ regulates LMP2/LMP7 and antigen processing via tyr (705)-p-STAT3 to affect autoimmunity*

Although STAT1/IRF can induce transcription of LMP2, LMP7 and MECL1 [37,41], it is not clear whether STAT3 directly regulates LMP2, LMP7 or MECL1. To address this, we analyzed the promoter sequences of human LMP2, LMP7, and MECL1 genes. Intriguingly, we found sequences highly homologous to the canonical STAT3 recognition motif TTCnnnGAA [39,42] in LMP2 and LMP7 promoter, but not in the MECL1 promoter. Luciferase reporter assay showed with increasing amounts of exogenous STAT3, LMP2- and LMP7-luc, but not MECL1-luc, activities were correspondingly elevated (Fig. 6A and Fig. S5A). In contrast, cells treated with Cucurbitacin E, an inhibitor of STAT3 phosphorylation (Fig. 6B), or silenced STAT3 (Fig. S5B), showed remarkably attenuated LMP2- and LMP7-luc activities. Both WT STAT3 and phosphorylation mimetic STAT3-Y705D significantly enhanced LMP2- and LMP7-luc activities, however phosphorylation-defective STAT3-Y705F can't (Fig. 6C). Expected changes in LMP2/LMP7 protein levels were observed after transfection of STAT3-Y705D/F constructs

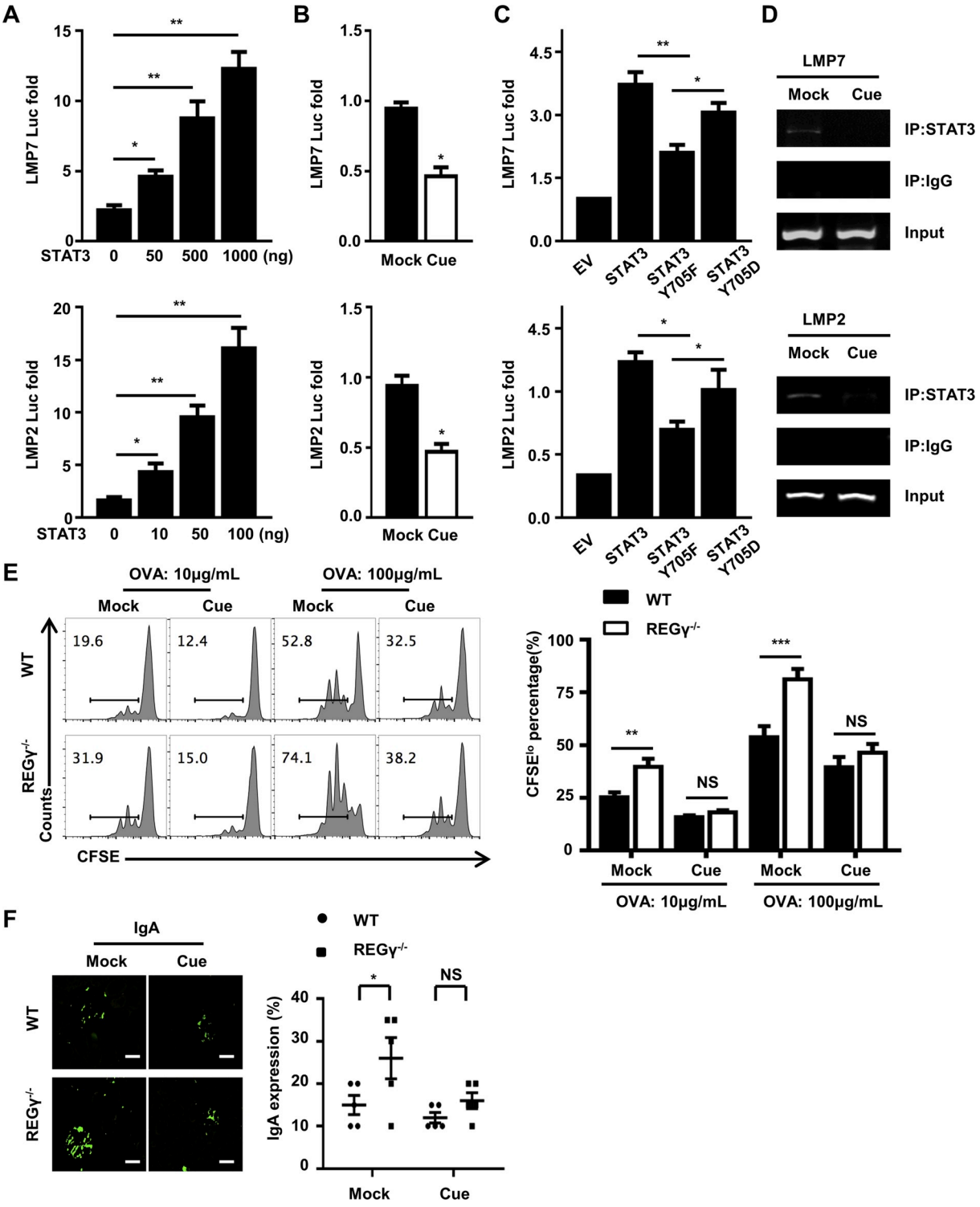


**Fig. 6. REGγ regulates LMP2/LMP7, antigen presentation and autoimmunity in a p-STAT3-dependant manner. (A)** 293T cells were co-transfected with LMP2 or LMP7 reporter constructs in combination with increasing amount of STAT3 plasmids for 24 h, followed by analysis of luciferase activity. **(B)** 293T cells were transfected with LMP2 or LMP7 reporter construct for 12 h, and then treated with STAT3 inhibitor 12 h and analyzed for luciferase activity. **(C)** 293T cells were co-transfected with LMP2 or LMP7 reporter constructs in combination with wild type, STAT3 (Y705D), or STAT3 (Y705F) plasmids, followed by analysis of luciferase activity. **(D)** BMDC cells were treated with mock or 500 nM Cucurbitacin E for 12 h, and Chromatin Immunoprecipitation was performed with indicated antibodies. **(E)** *REG*γ WT or KO BMDC cells were pretreated with 500 nM Cucurbitacin E for 12 h and then analyzed for their ability to stimulate the proliferation of $CD8^+$ T cells from OT-I mice. **(F)** 3-month-old wild type or *REG*$\gamma^{-/-}$ mice were treated with Cucurbitacin E every other day for 3 months and kidneys were sectioned for immunofluorescence staining. Magnification: 40x. Bar = 50 μm. Right panel showed the statistic results, *p < 0.05. (n = 5 mice for each genotype). In **(A-C, E)**, Statistical results were from 3 independent experiments. ***p < 0.001, **p < 0.01 and *p < 0.05 (two-tailed Student's t-test).

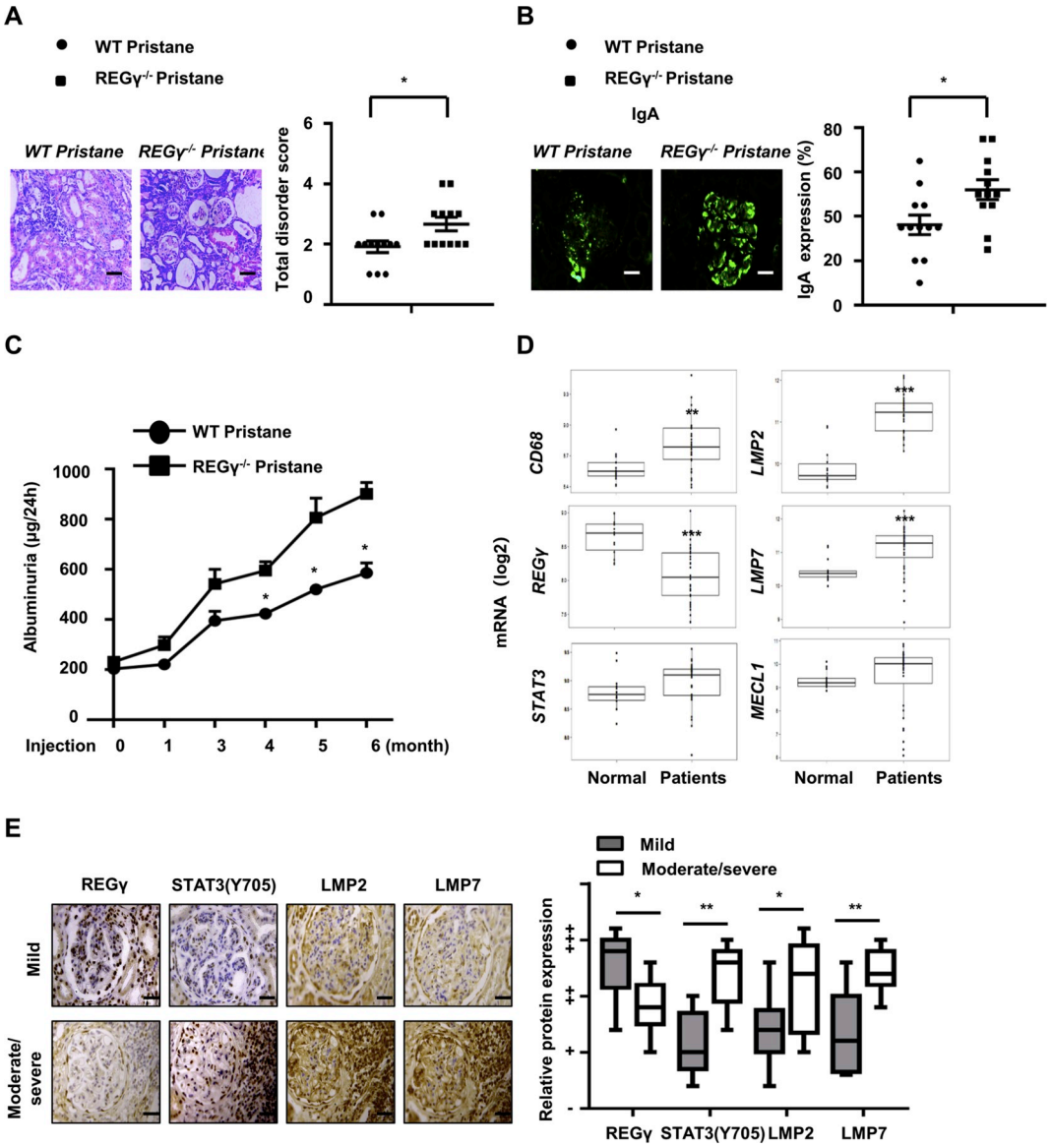


**Fig. 7. Function and expression of REGγ in mice and clinical SLE/LN patients.** 3-month-old of *REGγ*$^{+/+}$ (n = 12) or *REGγ*$^{-/-}$ (n = 12) mice were injected with Pristane and sacrificed the mice after 6 months, kidney tissue was removed for H&E staining **(A)** (Magnification: 20x. Bar = 100 μm) and (B) immunofluorescence staining IgA (Magnification: 40x. Bar = 50 μm). The statistical analysis results were shown as mean ± SEM. *p < 0.05 (two-tailed Student's t-test). **(C)** Mice were injected with Pristane for 6 months. At indicated time, albuminuria was measured by ELISA. The average was calculated based on three independent experiments with mean ± SEM. (Two-tailed Student's t-test, *p < 0.05). **(D)** Bioinformatic analysis of *REGγ*, *LMP2*, *LMP7*, *MECL-1* and *STAT3* mRNA levels in LN tissues (n = 32) compared with normal tissues (n = 14). **p < 0.01 and ***p < 0.001 (two-tailed Student's t-test). **(E)** Specimen from SLE/LN patients were collected for IHC analysis (Magnification: 40x. Bar = 50 μm. Right panel shows the statistical analysis) Tissue samples were collected from 13 cases with mild and 11 with moderate/severe manifestations. We define the type II lupus nephritis as the mild group, type III and IV as moderate/severe group. (Two-tailed Student's t-test, *p < 0.05, **p < 0.01).

(Fig. S5C). An increase of LMP2/LMP7 protein levels was seen with p-STAT3 in *REGγ*-deficient BMDC cells (Fig. S5D). However, elevation of LMP2/LMP7 proteins in *REGγ*$^{-/-}$ BMDC was abolished when cells were treated with STAT3 inhibitor Cucurbitacin E (Fig. S5E). Chromatin immunoprecipitation (Ch-IP) assays revealed a recruitment of STAT3 onto LMP2 and LMP7 promoters with mock treatment, but a decreased binding in the presence of Cucurbitacin E (Fig. 6D), indicating transcriptional regulation of LMP2 and LMP7 by phosphorylated STAT3. Cucurbitacin E treatment eliminated the differences in antigen presentation between *REGγ*$^{+/+}$ and *REGγ*$^{-/-}$ DC, as reflected by inhibition of CD8$^{+}$ T lymphocyte proliferation (Fig. 6E). Importantly, *REGγ*$^{-/-}$ mice treated with Cucurbitacin E markedly reduced deposition of IgA immune complex in kidney (Fig. 6F). These results demonstrate that REGγ affects immunoproteasome-dependent antigen processing and spontaneous autoimmunity via regulation of STAT3 activities.

### 3.7. *REGγ is clinically correlated with autoimmune disorder*

To further substantiate REGγ deficiency in promotion of autoimmunity, we expedited the development of autoimmune nephropathy in *REGγ*$^{-/-}$ mice by stimulation with Pristane, known to induce SLE-like kidney pathology in C57BL/6 mice [43]. Within 6 months of Pristane injection, *REGγ*$^{-/-}$ mice developed more severe autoimmune nephropathy (Fig. 7A), depositions of IgA (Fig. 7B), and albuminuria (Fig. 7C) than age-matched WT controls. These results further demonstrate that REGγ deficiency enhances autoimmune propensity.

To determine the clinical relevance of our discoveries, we analyzed

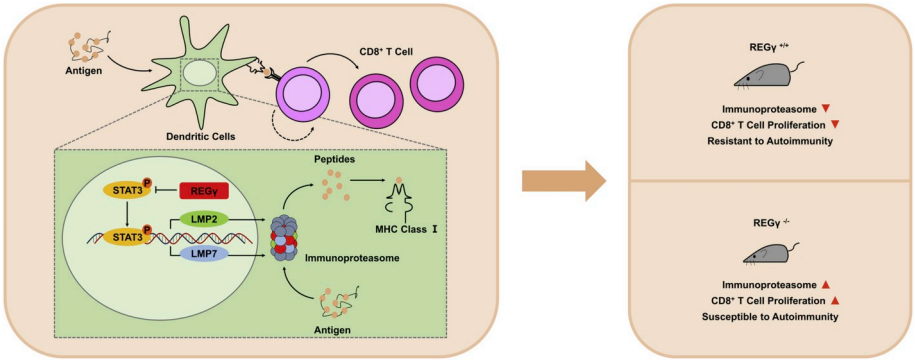


**Fig. 8.** Working model of the regulatory axis of REGγ—p-STAT3—LMP2/LMP7 in autoimmunity.

a public database (ID:GSE32591), including 32 cases of Lupus nephritis (LN) and 14 healthy glomerulus controls, for the expression profiles of REGγ, STAT3, LMP2, LMP7 and MECL1. We found that REGγ mRNA transcription was significantly lower in Lupus nephritis (CD68 as a marker). While LMP2 and LMP7 transcription was boosted, no dramatic change was observed in STAT3 and MECL1 mRNA levels (Fig. 7D). We substantiated the correlation among REGγ, STAT3, LMP2, and LMP7 in kidney tissues from 24 cases of LN patients by IHC analysis. REGγ expression was significantly lower in moderate/severe LN, whereas p-STAT3, LMP2, and LMP7 levels were higher in moderate/severe cases than in mild LN (Fig. 7E), implicating the regulatory axis of REGγ—p-STAT3—LMP2/LMP7 in autoimmune disease.

## 4. Discussion

We have demonstrated that REGγ is a new regulator that negatively controls the immunoproteasome and antigen presentation process. REGγ deficiency enhances stability of p-STAT3, which augments transcription of immunoproteasome subunits, and subsequently induces autoimmune symptoms. Based on this study and previous knowledge, we suggest a working model, in which p-STAT3 is translocated to the nucleus and transcriptionally activates the expression of immunoproteasome subunits LMP2 and LMP7. REGγ lowers p-STAT3 in the nucleus to downregulate LMP2/LMP7 expression, attenuating MHC I-restricted antigen processing and presentation to $CD8^+$ T cells (Fig. 8).

Immune response is altered with advancing age. On one hand, aging is characterized by an immunodeficiency or immunosenescence, which may lead to a decrease in the immune competence. On the other hand, inflammaging, an increased susceptibility to autoimmune responses and a persistent systemic inflammatory state, has been well documented in aged groups [44]. We have found that REGγ deficiency promotes aging [31]. In this study, we present several lines of evidence suggesting that REGγ may play roles in regulation of autoimmunity. First, REGγ can degrade p-STAT3 and decrease LMP2/LMP7 protein level in various types of cells, including HeLa, MEF, or DC cells either from young or old mice, suggesting a broad-spectrum protective role of REGγ in these cells (Fig. 1A and B; Fig. 4A and B; Fig. S1A, and Fig. S4A-C). Second, an obviously increased proliferation of $CD8^+$ T cells from OT-I mice has been found in 2-month old *REGγ*$^{-/-}$ mice upon OVA immunization (Fig. 2A–D). While without any specific immuno-stimulation, it took a longer time to observe the incremental number and percentage of $CD8^+$ T cells in *REGγ* knock-out mice (Fig. 2E). Third, we have observed significant autoimmune symptoms in elderly *REGγ*$^{-/-}$ mice (Fig. 3 and Fig. S3), and a depressed expression of REGγ in specimens from SLE/LN patients (Fig. 7D and E). Taken together, we believe that it is crucial to maintain REGγ expression or its activity at a "right" level. Reduced expression of REGγ may increase the probability for autoimmune disorders, both in aged mice without any infection, or in human LN. How REGγ levels are down regulated in LN is not clear and deserves further studies.

It is likely that autoimmune disorders in REGγ deficient mice may be contributed to by multiple mechanisms. As our data show, the alteration of immunoproteasome subunit MECL1 was detected at the protein level but not at mRNA level (Fig. 1 and Fig. S1). In correlation, we didn't see a marked increase in transcription of MECL1 by STAT3 (Fig. S5A), indicating that REGγ modulate MECL1 in a manner different from LMP2/LMP7. Aside from $CD8^+$ T cells, we observed that the DC percentage and cell number were elevated in *REGγ*$^{-/-}$ spleens (Fig. 2E). Although markedly increase serum ANA was observed in aged *REGγ*$^{-/-}$ mice, we didn't see major differences in cell number or percentage of $CD19^+$ B cells in WT mice versus *REGγ* KO mice (Figs. 2E and 3E). All these findings remain to be further studied.

Recently, bortezomib, the first FDA-approved proteasome inhibitor, has been successfully used in a patient with SLE and multiple myeloma [45,46]. Its use is limited because of the development of painful neuropathy in > 30% of patients [47]. Thus, developing less toxic proteasome inhibitors is important. A promising LMP7-specific inhibitor, PR-957, is equally efficacious and less toxic in several autoimmune disease mice models than bortezomib [19,20,48]. Our results provide new insights for targeting STAT3—LMP2/LMP7 in autoimmune disorders.

## 5. Conclusions

REGγ functions as a check point to maintain p-STAT3 at steady-state level, counterbalance the immunoproteasome and affect autoimmunity.

## Declaration of interest

The authors have declared that no conflict of interest exists.

## Author contributions

XTL, BHZ, JRX, and LL designed research. LFY, LZ, and YX performed the molecular and cell biology, immunological, and animal experiments, respectively. PZ provided clinical samples and performed data analysis. TZW, YYX, XQM, ASS and RM were involved in the molecular and cell biology study. XSW, WX and HYW contributed to the immunological work. SWS, TYM, YYX and XLM contributed to the animal work. HW contributed to data analysis. XTL, BHZ, and LFY wrote the paper.

## Acknowledgements

This work was supported by the National Program on Key Basic Research Project (973 Program) (2015CB901402), the National Natural Science Foundation of China (31670882, 31100946, 91629103, 81471066, 81261120555, 81672883, 81401837, 31071875, 31200878), the Science and Technology Commission of Shanghai

Municipality (16ZR1410000, 14430712100, 11ZR1410000, 16QA1401500).

We also thank ECNU Multifunctional Platform for Innovation (011) for keeping and raising mice.

## Appendix A. Supplementary data

Supplementary data to this article can be found online at https://doi.org/10.1016/j.jaut.2019.05.010.

When REGγ expression is high, the phosphrylated-STAT3 can be directly degraded by the REGγ-20S proteasome, resulting in lower expression of immunoproteasome subunits and activity. Thus the antigen processing and presentation are limited. Conversely, when the REGγ level is low, the phosphrylated-STAT3 can translocate into the nucleus and bind to the promoter region of LMP2 and LMP7, activating transcription of these genes. Consequently, the immunoproteasome activity and the processing and presentation of MHC-I restricted antigen to the $CD8^+$ T cells are enhanced, which may cause autoimmune symptoms.

## References

[1] L. Van Kaer, P.G. Ashton-Rickardt, M. Eichelberger, M. Gaczynska, K. Nagashima, K.L. Rock, et al., Altered peptidase and viral-specific T cell response in LMP2 mutant mice, Immunity 1 (1994) 533–541.
[2] P. Leone, E.C. Shin, F. Perosa, A. Vacca, F. Dammacco, V. Racanelli, MHC class I antigen processing and presenting machinery: organization, function, and defects in tumor cells, J. Natl. Cancer Inst. 105 (2013) 1172–1187.
[3] J.P. Mackern-Oberti, C. Llanos, F. Vega, F. Salazar-Onfray, C.A. Riedel, S.M. Bueno, et al., Role of dendritic cells in the initiation, progress and modulation of systemic autoimmune diseases, Autoimmun. Rev. 14 (2015) 127–139.
[4] L.J. Carreno, R. Pacheco, M.A. Gutierrez, S. Jacobelli, A.M. Kalergis, Disease activity in systemic lupus erythematosus is associated with an altered expression of low-affinity Fc gamma receptors and costimulatory molecules on dendritic cells, Immunology 128 (2009) 334–341.
[5] D.M. Gravano, K.K. Hoyer, Promotion and prevention of autoimmune disease by CD8+ T cells, J. Autoimmun. 45 (2013) 68–79.
[6] F. Giovanni, P. Domenico, M. Alessandro, I. Raffaele, N. Viviana, P.A. Katia, et al., Circulating CD8+CD56-perforin+ T cells are increased in multiple sclerosis patients, J. Neuroimmunol. 240-241 (2011) 137–141.
[7] Q. Ji, A. Perchellet, J.M. Goverman, Viral infection triggers central nervous system autoimmunity via activation of CD8+ T cells expressing dual TCRs, Nat. Immunol. 11 (2010) 628–634.
[8] S. Sinha, A.W. Boyden, F.R. Itani, M.P. Crawford, N.J. Karandikar, CD8(+) T-cells as immune regulators of multiple sclerosis, Front. Immunol. 6 (2015) 619.
[9] M. Yang, C. Peyret, X.Q. Shi, N. Siron, J.H. Jang, S. Wu, et al., Evidence from human and animal studies: pathological roles of CD8(+) T cells in autoimmune peripheral neuropathies, Front. Immunol. 6 (2015) 532.
[10] S.J. Smirnova, J.V. Sidorova, N.V. Tsvetaeva, O.F. Nikulina, B.V. Biderman, E.E. Nikulina, et al., Expansion of CD8+ cells in autoimmune hemolytic anemia, Autoimmunity 49 (2016) 147–154.
[11] Y.M. Kang, X. Zhang, U.G. Wagner, H. Yang, R.D. Beckenbaugh, P.J. Kurtin, et al., CD8 T cells are required for the formation of ectopic germinal centers in rheumatoid synovitis, J. Exp. Med. 195 (2002) 1325–1336.
[12] J. Lowe, D. Stock, B. Jap, P. Zwickl, W. Baumeister, R. Huber, Crystal Structure of the 20S Proteasome from the Archaeon T. Acidophilum at 3.4 A Resolution, vol. 268, Science, New York, NY), 1995, pp. 533–539.
[13] L.F. Barton, M. Cruz, R. Rangwala, G.S. Deepe Jr., J.J. Monaco, Regulation of immunoproteasome subunit expression in vivo following pathogenic fungal infection, J. Immunol. 169 (2002) 3046–3052.
[14] M. Groettrup, S. Standera, R. Stohwasser, P.M. Kloetzel, The subunits MECL-1 and LMP2 are mutually required for incorporation into the 20S proteasome, Proc. Natl. Acad. Sci. U. S. A 94 (1997) 8970–8975.
[15] E.C. Shin, U. Seifert, T. Kato, C.M. Rice, S.M. Feinstone, P.M. Kloetzel, et al., Virus-induced type I IFN stimulates generation of immunoproteasomes at the site of infection, J. Clin. Investig. 116 (2006) 3006–3014.
[16] T.A. Griffin, D. Nandi, M. Cruz, H.J. Fehling, L.V. Kaer, J.J. Monaco, et al., Immunoproteasome assembly: cooperative incorporation of interferon gamma (IFN-gamma)-inducible subunits, J. Exp. Med. 187 (1998) 97–104.
[17] A. Macagno, M. Gilliet, F. Sallusto, A. Lanzavecchia, F.O. Nestle, M. Groettrup, Dendritic cells up-regulate immunoproteasomes and the proteasome regulator PA28 during maturation, Eur. J. Immunol. 29 (1999) 4037–4042.
[18] E.Z. Kincaid, J.W. Che, I. York, H. Escobar, E. Reyes-Vargas, J.C. Delgado, et al., Mice completely lacking immunoproteasomes show major changes in antigen presentation, Nat. Immunol. 13 (2011) 129–135.
[19] T. Muchamuel, M. Basler, M.A. Aujay, E. Suzuki, K.W. Kalim, C. Lauer, et al., A selective inhibitor of the immunoproteasome subunit LMP7 blocks cytokine production and attenuates progression of experimental arthritis, Nat. Med. 15 (2009) 781–787.
[20] H.T. Ichikawa, T. Conley, T. Muchamuel, J. Jiang, S. Lee, T. Owen, et al., Beneficial effect of novel proteasome inhibitors in murine lupus via dual inhibition of type I interferon and autoantibody-secreting cells, Arthritis Rheum. 64 (2012) 493–503.
[21] Y. Nagayama, M. Nakahara, M. Shimamura, I. Horie, K. Arima, N. Abiru, Prophylactic and therapeutic efficacies of a selective inhibitor of the immunoproteasome for Hashimoto's thyroiditis, but not for Graves' hyperthyroidism, in mice, Clin. Exp. Immunol. 168 (2012) 268–273.
[22] M. Basler, S. Mundt, T. Muchamuel, C. Moll, J. Jiang, M. Groettrup, et al., Inhibition of the immunoproteasome ameliorates experimental autoimmune encephalomyelitis, EMBO Mol. Med. 6 (2014) 226–238.
[23] N. Vigneron, B.J. Van den Eynde, Proteasome subtypes and regulators in the processing of antigenic peptides presented by class I molecules of the major histocompatibility complex, Biomolecules 4 (2014) 994–1025.
[24] S. Murata, H. Udono, N. Tanahashi, N. Hamada, K. Watanabe, K. Adachi, et al., Immunoproteasome assembly and antigen presentation in mice lacking both PA28alpha and PA28beta, EMBO J. 20 (2001) 5898–5907.
[25] N. Tanahashi, K. Yokota, J.Y. Ahn, C.H. Chung, T. Fujiwara, E. Takahashi, et al., Molecular properties of the proteasome activator PA28 family proteins and gamma-interferon regulation, Genes Cells 2 (1997) 195–211.
[26] T. Preckel, W.P. Fung-Leung, Z. Cai, A. Vitiello, L. Salter-Cid, O. Winqvist, et al., Impaired immunoproteasome assembly and immune responses in PA28-/- mice, Science 286 (1999) 2162–2165 (New York, NY).
[27] X. Li, D.M. Lonard, S.Y. Jung, A. Malovannaya, Q. Feng, J. Qin, et al., The SRC-3/AIB1 coactivator is degraded in a ubiquitin- and ATP-independent manner by the REGgamma proteasome, Cell 124 (2006) 381–392.
[28] X. Li, L. Amazit, W. Long, D.M. Lonard, J.J. Monaco, B.W. O'Malley, Ubiquitin- and ATP-independent proteolytic turnover of p21 by the REGgamma-proteasome pathway, Mol. Cell 26 (2007) 831–842.
[29] X. Chen, L.F. Barton, Y. Chi, B.E. Clurman, J.M. Roberts, Ubiquitin-independent degradation of cell-cycle inhibitors by the REGgamma proteasome, Mol. Cell 26 (2007) 843–852.
[30] Y. Uchimura, L.F. Barton, C. Rada, M.S. Neuberger, REG-gamma associates with and modulates the abundance of nuclear activation-induced deaminase, J. Exp. Med. 208 (2011) 2385–2391.
[31] L. Li, D. Zhao, H. Wei, L. Yao, Y. Dang, A. Amjad, et al., REGgamma deficiency promotes premature aging via the casein kinase 1 pathway, Proc. Natl. Acad. Sci. U. S. A 110 (2013) 11005–11010.
[32] J. Liu, G. Yu, Y. Zhao, D. Zhao, Y. Wang, L. Wang, et al., REGgamma modulates p53 activity by regulating its cellular localization, J. Cell Sci. 123 (2010) 4076–4084.
[33] M. Rechsteiner, C. Realini, V. Ustrell, The proteasome activator 11 S REG (PA28) and class I antigen presentation, Biochem. J. 345 (Pt 1) (2000) 1–15.
[34] L.F. Barton, H.A. Runnels, T.D. Schell, Y. Cho, R. Gibbons, S.S. Tevethia, et al., Immune defects in 28-kDa proteasome activator gamma-deficient mice, J. Immunol. 172 (2004) 3948–3954.
[35] M.A. Alikhan, M. Huynh, A.R. Kitching, J.D. Ooi, Regulatory T cells in renal disease, Clin Transl Immunol. 7 (2018) e1004.
[36] Y. Lv, B. Meng, H. Dong, T. Jing, N. Wu, Y. Yang, et al., Upregulation of GSK3beta contributes to brain disorders in elderly REGgamma-knockout mice, Neuropsychopharmacology 41 (2016) 1340–1349.
[37] M. Chatterjee-Kishore, R. Kishore, D.J. Hicklin, F.M. Marincola, S. Ferrone, Different requirements for signal transducer and activator of transcription 1alpha and interferon regulatory factor 1 in the regulation of low molecular mass polypeptide 2 and transporter associated with antigen processing 1 gene expression, J. Biol. Chem. 273 (1998) 16177–16183.
[38] J. Xu, L. Zhou, L. Ji, F. Chen, K. Fortmann, K. Zhang, et al., The REGgamma-proteasome forms a regulatory circuit with IkappaBvarepsilon and NFkappaB in experimental colitis, Nat. Commun. 7 (2016) 10761.
[39] S. Abroun, N. Saki, M. Ahmadvand, F. Asghari, F. Salari, F. Rahim, STATs: an old story, yet mesmerizing, Cell J. 17 (2015) 395–411.
[40] C. Wojcik, K. Tanaka, N. Paweletz, U. Naab, S. Wilk, Proteasome activator (PA28) subunits, alpha, beta and gamma (Ki antigen) in NT2 neuronal precursor cells and HeLa S3 cells, Eur. J. Cell Biol. 77 (1998) 151–160.
[41] C.H. Chang, J. Hammer, J.E. Loh, W.L. Fodor, R.A. Flavell, The activation of major histocompatibility complex class I genes by interferon regulatory factor-1 (IRF-1), Immunogenetics 35 (1992) 378–384.
[42] A.P. Hutchins, S. Poulain, D. Miranda-Saavedra, Genome-wide analysis of STAT3 binding in vivo predicts effectors of the anti-inflammatory response in macrophages, Blood 119 (2012) e110–e119.
[43] W.H. Reeves, P.Y. Lee, J.S. Weinstein, M. Satoh, L. Lu, Induction of autoimmunity by pristane and other naturally occurring hydrocarbons, Trends Immunol. 30 (2009) 455–464.
[44] S. Sotgia, A. Zinellu, A.A. Mangoni, R. Serra, G. Pintus, C. Caruso, et al., Cellular immune activation in Sardinian middle-aged, older adults and centenarians, Exp. Gerontol. 99 (2017) 133–137.
[45] R.C. Kane, P.F. Bross, A.T. Farrell, R. Pazdur, U.S. Velcade, FDA approval for the treatment of multiple myeloma progressing on prior therapy, Oncol. 8 (2003) 508–513.
[46] K. Frohlich, J.U. Holle, P.M. Aries, W.L. Gross, F. Moosig, Successful use of bortezomib in a patient with systemic lupus erythematosus and multiple myeloma, Ann. Rheum. Dis. 70 (2011) 1344–1345.
[47] A. Badros, O. Goloubeva, J.S. Dalal, I. Can, J. Thompson, A.P. Rapoport, et al., Neurotoxicity of bortezomib therapy in multiple myeloma: a single-center experience and review of the literature, Cancer 110 (2007) 1042–1049.
[48] M. Basler, M. Dajee, C. Moll, M. Groettrup, C.J. Kirk, Prevention of experimental colitis by a selective inhibitor of the immunoproteasome, J. Immunol. 185 (2010) 634–641.